BRCA2 deficiency in mice leads to meiotic impairment and infertility

Shyam K. Sharan[1,*], April Pyle[2], Vincenzo Coppola[1], Janice Babus[3], Srividya Swaminathan[1], Jamie Benedict[3], Deborah Swing[1], Betty K. Martin[1], Lino Tessarollo[1], Janice P. Evans[4], Jodi A. Flaws[3] and Mary Ann Handel[2]

[1]Mouse Cancer Genetics Program, Center for Cancer Research, National Cancer Institute at Frederick, 1050 Boyles Street, Frederick, MD 21702, USA
[2]Department of Biochemistry and Cellular and Molecular Biology, University of Tennessee, Knoxville, TN 37996, USA
[3]Department of Epidemiology and Preventive Medicine, School of Medicine, University of Maryland, Baltimore, MD 21201, USA
[4]Department of Biochemistry and Molecular Biology, Division of Reproductive Biology, Johns Hopkins University, Bloomberg School of Public Health, Baltimore, MD 21205, USA
*Author for correspondence (e-mail: ssharan@mail.ncifcrf.gov)

Accepted 29 September 2003

Development 131, 131-142
Published by The Company of Biologists 2004
doi:10.1242/dev.00888

Summary

The role of *Brca2* in gametogenesis has been obscure because of embryonic lethality of the knockout mice. We generated *Brca2*-null mice carrying a human BAC with the *BRCA2* gene. This construct rescues embryonic lethality and the mice develop normally. However, there is poor expression of the transgene in the gonads and the mice are infertile, allowing examination of the function of BRCA2 in gametogenesis. BRCA2-deficient spermatocytes fail to progress beyond the early prophase I stage of meiosis. Observations on localization of recombination-related and spermatogenic-related proteins suggest that the spermatocytes undergo early steps of recombination (DNA double strand break formation), but fail to complete recombination or initiate spermiogenic development. In contrast to the early meiotic prophase arrest of spermatocytes, some mutant oocytes can progress through meiotic prophase I, albeit with a high frequency of nuclear abnormalities, and can be fertilized and produce embryos. Nonetheless, there is marked depletion of germ cells in adult females. These studies provide evidence for key roles of the BRCA2 protein in mammalian gametogenesis and meiotic success.

Key words: BRCA2, Spermatogenesis, Oogenesis, Meiosis, DNA repair

Introduction

Since the cloning of the human breast cancer susceptibility genes *BRCA1* and *BRCA2*, their roles in various biological processes has been extensively investigated (reviewed by Venkitaraman, 2002). Although it is well known that mutations in these genes predispose individuals to breast and ovarian cancer (Rahman and Stratton, 1998), the roles of the BRCA1 and BRCA2 proteins in other biological processes are not fully understood. Both BRCA1 and BRCA2 proteins have been implicated in DNA repair processes. The BRCA2 protein consists of 3418 amino acids with no clearly defined functional domains (Wooster et al., 1995; Tavtigian et al., 1996). Sequence analysis revealed presence of eight novel internal repetitive units, the 'BRC-repeats' (Bork et al., 1996). A role for BRCA2 in DNA repair became evident when its interaction with the DNA repair protein RAD51 was identified (Sharan et al., 1997; Patel et al., 1998). The C terminus of the BRCA2 protein and six out of the eight BRC repeats was shown to directly interact with RAD51 (Sharan et al., 1997; Wong et al., 1997). A recent investigation of the crystal structure of the C terminus of BRCA2 revealed the presence of several single-stranded DNA-binding motifs, suggesting that BRCA2 could bind directly to DNA and stimulate RAD51 mediated recombination (Yang et al., 2002). Studies showing its upregulation in rapidly dividing cells, and its cell-cycle dependent expression peaking at the G_1/S boundary, suggest that BRCA2 may be involved in cell-cycle regulation (Rajan et al., 1996; Vaughn et al., 1996).

The involvement of *BRCA1* and *BRCA2* mutations in human ovarian cancer as well as the possible roles of the proteins in DNA dynamics has suggested the possibility that breast cancer susceptibility genes may function during normal gametogenesis. Until recently, evidence supporting this idea has derived primarily from expression studies. In mice, both *Brca1* and *Brca2* are expressed during spermatogenesis, particularly during meiotic prophase (Zabludoff et al., 1996; Blackshear et al., 1998; Chen et al., 1998). Intriguingly, the BRCA2 protein is localized on meiotic chromosomes (Chen et al., 1998), suggesting a role in the dynamics of meiotic recombination and/or chromosome pairing and synapsis.

However, the role of BRCA2 in meiosis and gametogenesis has been difficult to define because loss-of-function mutations in the mouse *Brca2* gene result in early embryonic lethality (Hakem et al., 1998). We report a viable but infertile mouse model with impaired BRCA2 expression. The mutant mice lack endogenous *Brca2* function but carry a human *BRCA2* gene present in a bacterial artificial chromosome (BAC). The human transgene rescues the embryonic lethality phenotype of the *Brca2*-null mice; however, there is poor expression of the human *BRCA2* transgene in the testes and ovaries, with ensuing

infertility. We use this mouse model to define stages of gametogenesis impaired by deficient BRCA2 expression and find evidence for a role in meiosis and gametogenic success in both males and females.

Materials and methods

Isolation and characterization of BACs

Human genomic BAC library filters obtained from Roswell Park Cancer Institute (now available at BACPAC Resource Center at the Children's Hospital Oakland Research Institute in Oakland, California) were screened using probes derived from PCR amplified DNA fragments from the 5′ (nucleotides 331-850) and 3′ (nucleotides 9852-10420) ends of the human *BRCA2* cDNA (NM 000059). Thirteen clones were obtained from the human BAC library and seven were hybridized to both end probes. To identify the clone with the largest upstream and downstream regions, the T7 and SP6 ends of each BAC clone were sequenced and compared with the published sequence of human *BRCA2* region. Human *BRCA2* BAC, RP11-777I19 was selected to generate transgenic mice. The insert size (~165 kb) was confirmed by pulsed field gel electrophoresis of *Not*I-digested BAC DNA.

Generation of BAC transgenic mice

BAC DNA was extracted using standard alkaline lysis and purification on a cesium chloride gradient. Supercoiled DNA was dialyzed overnight in 1×TE (10mM Tris pH 7.6, 1mM EDTA) and diluted to 0.5-1.0 ng/μl for pronuclear microinjection. Pronuclear microinjection was performed as described by Hogan et al. (Hogan et al., 1994).

Genotyping mice by Southern analysis and genetic crosses

Transgenic mice were identified by Southern analysis of *Bam*HI digested tail DNA using the chloramphenicol resistance gene present in the BAC vector as a probe to detect a 8.0 kb fragment. *Brca2* heterozygous and homozygous mutant mice were genotyped by hybridizing *Eco*RV digested genomic DNA on a Southern blot with a 1.5 kb fragment from exon 11 of murine *Brca2* gene nucleotides 5208-6710 of NM 009765. The probe detects a 5 kb wild-type fragment and a 6.5 kb fragment corresponding to the mutant allele. BAC transgenic founders were crossed with *Brca2 Ko/+* mice to obtain *Brca2 Ko/+;Tg/+* F1 progeny. The *Brca2 Ko/+;Tg/+* F1 mice were crossed to *Brca2 Ko/+* mice to obtain *Brca2 Ko/Ko;Tg/+* mice.

Expression analysis by in situ hybridization

E9.5 and E11.5 embryos, ovaries and testes were fixed in freshly prepared 4% paraformaldehyde and embedded in paraffin wax for sectioning. In situ hybridization was performed as described by Tessarollo and Parada (Tessarollo and Parada, 1995).

Probes

PCR fragments containing regions of mouse *Brca2* (nucleotides 9500-10129, NM 009765) and human *BRCA2* (nucleotides 10141-10770, NM 000059) cDNA were cloned into the *pGEM-T* vector (Promega) and sequenced to determine their orientation. ^{35}S-labeled-antisense human *BRCA2* and mouse *Brca2* probes were generated by in vitro transcription using T7 RNA polymerase and *Not*I linearized template. The corresponding sense probes were generated using SP6 RNA polymerase and *Nco*I (mouse *Brca2*) or *Sac*II (human *BRCA2*) linearized templates. In situ hybridization was performed in triplicate for each sample and the experiments were repeated at least once to evaluate the consistency of the results.

Histology

E9.5 and E11.5 embryos, testes and ovaries were fixed in Bouin's solution. Samples were dehydrated through an ethanol series, embedded in paraffin wax, serially sectioned and stained with Hematoxylin and Eosin. Histological sections of testes were stained with periodic acid Schiff (PAS)-Hematoxylin and the ovaries from postnatal day 2 pups were stained with Weigert's Hematoxylin-picric acid Methyl Blue. Slides were examined using brightfield microscopy. To examine the consistency of the phenotype, samples from at least two different mice were examined with the exception of the testis from a 7-month-old mouse where a single male was examined.

Cell death assay

A TUNEL assay (In Situ Cell Death detection kit, Roche Molecular Biochemicals) was performed according to the manufacturer's instructions on testes of 3-week-old mice. Testes were fixed in 4% paraformaldehyde and processed as described by Tessarollo and Parada (Tessarollo and Parada, 1995). Anti-fluorescein antibody conjugated with horse-radish peroxidase (POD) was used to detect fluorescein labeled dUTP. DAB substrate (Roche Molecular Biochemicals) was used to detect POD and visualized by light microscopy.

Fixation and immunofluorescent labeling of isolated germ cells

Cell preparations enriched in germ cells were prepared as previously described (Cobb et al., 1999). Briefly, testes were detunicated and digested in 0.5 mg/ml collagenase (Sigma) in Krebs-Ringer buffer for 20 minutes at 32°C and then in 0.5 mg/ml trypsin (Sigma) for 13 minutes, followed by filtering through 80 μm Nitex mesh and washing in buffer. Surface-spread preparations were used to visualize nuclei as previously described (Cobb et al., 1997). Cell preparations from at least two rescued mice were used for each antibody staining.

Antisera used were polyclonal human BRCA2 antibody, Ab-2 (Oncogene Research, 1:50), anti-mouse BRCA2 (Pep-3, polyclonal antisera against mouse BRCA2 amino acids 2330-2345, 1:50), anti-SYCP3 (1:500) (Eaker et al., 2001), anti-SPO11 (Trevigen, 1:25), anti-DMC1 (Masson et al., 1999) (a generous gift from Madalena Tarsounas and Stephen West, Cancer Research UK), anti-RAD51 (Oncogene 1:100), anti-H1t (polyclonal antisera raised against full-length H1t cDNA, 1:1000), anti-γH2AX (Upstate; Lake Placid, NY, 1:500) and anti-RPA (Oncogene 1:25). After overnight incubation in primary antibody, slides were incubated with rhodamine- or fluorescein-conjugated secondary antibodies (Pierce, 1:500), followed by mounting with Prolong Antifade (Molecular Probes) containing DAPI (Molecular Probes) to stain DNA. Control slides were stained with either secondary antibodies only, or pre-immune sera to replace primary antibody. Localization was observed with an Olympus epifluorescence microscope and images were captured and transferred to Adobe PhotoShop with a Hamamatsu color 3CCD camera.

Follicular count

Quantitative analysis of ovarian follicles was completed by marking every tenth section and counting the total number of primordial, primary, preantral and antral follicles present in each of these marked sections. Follicles were counted as primordial if they contained an intact oocyte and were surrounded by a single layer of flattened granulosa cells. Follicles were counted as primary if they contained an intact oocyte and were surrounded by a single layer of cuboidal shaped granulosa cells; as preantral if they contained an intact oocyte, more than one layer of granulose cells and lacked antral spaces; and as antral if they contained an intact oocyte, more than one layer of granulosa cells and antral spaces. To avoid double-counting follicles, only follicles containing an oocyte with a visible nucleus were counted. The number of follicles was multiplied by 10 to account for the fact that every tenth section was used in the analysis (Smith et al., 1991). To avoid bias, all ovaries were analyzed without knowledge of genotype or age.

Superovulation

Females were superovulated and oocytes were collected as described by Hogan et al. (Hogan et al., 1994). Briefly, 0.1 ml of PMS (5 IU) was injected into the intraperitoneal cavity of 6-week-old females. After 46 hours, 0.1 ml of hCG (5 IU) was injected into each female. After 18 hours the females were sacrificed and the oviducts were dissected out. The oviducts were opened with fine forceps and the eggs were collected. Cumulus cells were dissociated in presence of 700 units/ml of hyaluronidase.

In vitro oocyte maturation

Forty-eight hours after PMSG injection, germinal vesicle (GV)-intact oocytes were collected from ovarian follicles by piercing the ovaries of two control and two rescue mice (7 and 9 weeks of age) with 27.5 gauge syringe needles in Whitten's medium containing 0.05% polyvinyl alcohol (Sigma, St. Louis, MO) and 0.25 mM dibutyryl cAMP (dbcAMP, Sigma) (Cho et al., 1974). All oocytes collected, those enclosed in cumulus cells and those not enclosed in cumulus cells, were used in studies of in vitro maturation. For those oocytes that emerged from follicles enclosed in cumulus cells, the cumulus cells were removed by pipetting the oocyte-cumulus cell complexes through a thin-bore pipet. GV-intact oocytes were matured in vitro by washing the oocytes through six 100 μl drops of Whitten's medium lacking dbcAMP, and then cultured overnight at 37°C in 100 μl drops Whitten's medium (10-25 oocytes per drop) in 5% CO_2 in air. At 16 hour post-dbcAMP removal, the cells were viewed by dissecting microscope to assess what percentage of the oocytes had emitted the first polar body (PB1), undergone GV breakdown (GVBD) but not emitted PB1, were still GV intact, or had other phenotypes. Less than 50% of the control oocytes had emitted the first polar body by this time. As oocytes of some strains of mice undergo meiotic maturation more slowly than others (Polanski et al., 1998), we cultured these oocytes for additional 3 hours to 19 hours post-dbcAMP removal. Some oocytes remained GV intact after these 19 hours [27% (22/81), control; 14% (4/29)]; this might be attributable to the use of all oocytes collected (i.e. potentially including some meiotically incompetent oocytes) in these maturation studies. At 19 hour post-dbcAMP removal, the cells were prepared for staining as follows. The zonae pellucidae were removed by a brief incubation in acidic medium-compatible buffer (10 mM HEPES, 1 mM NaH_2PO_4, 0.8 mM $MgSO_4$, 5.4 mM KCl, 116.4 mM NaCl, final pH 1.5), and then the cells were fixed in freshly prepared 3.7% paraformaldehyde in PBS for 1-2 hours. Fixation and all subsequent steps were performed at room temperature in a humidified chamber as described previously (Evans et al., 2000). The fixed cells were washed in PBS, then permeabilized in PBS containing 0.1% Triton X-100 for 15 minutes, and then incubated in blocking solution (PBS containing 0.1% BSA and 0.01% Tween-20) for 60 minutes. Cells were stained with 50 ng/ml of TRITC-conjugated phalloidin (Sigma) for 45 minutes to label F-actin. Cells were then washed three times (in blocking solution, 10-20 minutes each), and then mounted in VectaShield mounting medium (Vector Labs; Burlingame, CA) containing 1.5 μg/ml 4′,6-diamidino-2-phenylindole (DAPI; Sigma). Cells were viewed on a Nikon Eclipse fluorescent microscope, and digital images were captured with a Princeton 5 MHz cooled interlined CCD camera (Princeton Instruments, Trenton, NJ) using IP Labs software (Scanalytics, Fairfax, VA). All images were collected with similar exposure times and were not further manipulated, except for cropping in Photoshop 6.0 (Adobe systems Incorporated, San Jose, CA) for figure preparation. Throughout this work, the term 'oocyte' refers to GV-intact oocytes at prophase I; the term 'egg' refers to a metaphase II egg.

Results

Generation of transgenic mice using human *BRCA2*

A BAC clone containing full-length human *BRCA2* gene was obtained from a genomic library generated in BAC vector pBACe3.6. The BAC clone, RP11-777I19, with a 165 kb insert that included the 80 kb *BRCA2* gene and 30 kb of upstream and 55 kb of downstream region, was used to generate transgenic mice (Fig. 1A). Four founder transgenic mice carrying one to three copies of the BAC (data not shown) were then crossed to mice heterozygous for a mutant allele of *Brca2*. The heterozygous mice (*Brca2*^{Brdm1}/+, in brief represented as *Brca2 Ko*/+) are viable and fertile, whereas the homozygous mutant (designated as *Brca2 Ko/Ko*) embryos die during development around E7.5 (Sharan et al., 1997). The expression of the human transgene in multiple tissues was examined in 6- to 8-week-old *Brca2* heterozygous transgenic F1 (*Brca2 Ko/+; TgN(RP11-777I19)1sks/+*, in brief represented as *Brca2 Ko/+; Tg/+*) animals by RT-PCR. Of the four lines that were examined, only one showed expression of the human gene (data not shown).

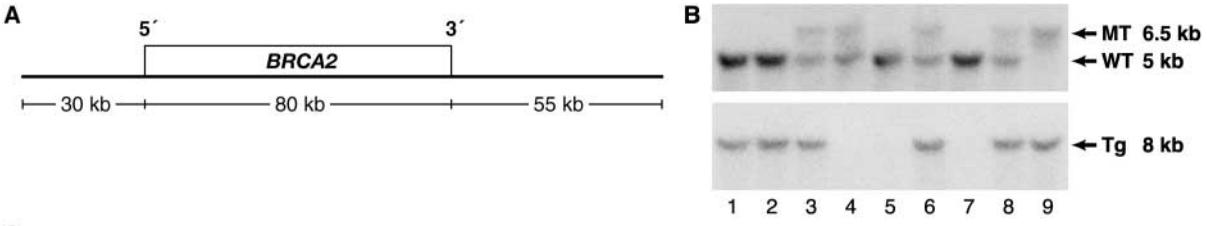

C

Genotype:	+/+	+/+; Tg/+	Brca2 Ko/+	Brca2 Ko/+; Tg/+	Brca2 Ko/Ko	Brca2 Ko/Ko; Tg/+
Observed	38	31	86	83	0	33
Expected	38.7	38.7	77.4	77.4	0	38.7

Fig. 1. (A) The 165 kb BAC RP11-777I19 insert. The insert contains 80 kb of the *BRCA2* gene as well as 30 kb of the upstream region and 55 kb of the flanking downstream region. In addition to *BRCA2*, based on the sequence information (Accession Numbers Z73359 and 74739) the BAC insert is predicted to contain two novel genes of unknown function. (B) Southern analysis of *Eco*RV digested DNA isolated from littermates obtained from a cross between *Brca2 Ko/+; Tg/+* and *Brca2 Ko/+* mice. WT, wild-type allele; MT, mutant allele. Presence of a 8 kb band (lower panel) on *Bam*HI-digested DNA shows the presence of the BAC transgene (Tg); (C) Table showing the offspring of various genotypes obtained from a cross between *Brca2 Ko/+; Tg/+* and *Brca2 Ko/+* mice, in expected Mendelian ratios.

The *Brca2 Ko/+; Tg/+* mice were crossed to *Brca2 Ko/+* mice, producing *Brca2 Ko/Ko*; *Tg/+* mice (Fig. 1B). These rescued homozygous mutant mice were viable and morphologically indistinguishable from their littermates. The mutant mice were obtained in the expected Mendelian ratio (P=0.59) (Fig. 1C), suggesting no embryonic lethality. The three lines that did not express the human *BRCA2* gene failed to rescue the lethality of the *Brca2* homozygous embryos (data not shown). The observation that the *BRCA2* transgene rescued embryonic lethality of the homozygous mutant mice suggests that the human gene is functional in mice. However, the rescued mice failed to produce offspring when intercrossed. When the *Brca2 Ko/Ko*; *Tg/+* mice were crossed to wild-type mice, both wild-type and rescued females showed presence of copulatory plugs. However, neither *Brca2 Ko/Ko*; *Tg/+* females nor wild-type females mated to *Brca2 Ko/Ko*; *Tg/+* males produced any pups, suggesting that both *Brca2 Ko/Ko*; *Tg/+* males and females were infertile. The fact that *Brca2 Ko/+; Tg/+* mice are fertile strongly suggests that the infertility of the *Brca2 Ko/Ko; Tg/+* mice is not due solely to a deleterious effect of the BAC, but is caused by loss of endogenous BRCA2 protein function.

Expression of the endogenous *Brca2* gene and the human *BRCA2* transgene

To investigate the rescue of embryonic lethality by the human *BRCA2*-containing BAC, the expression of the human transgene was examined by RT-PCR. Although the level of expression of the human gene appeared lower than that of the endogenous *Brca2* gene, the two exhibited qualitatively identical expression patterns revealed by RT-PCR. Both were expressed in brain, heart, liver, lung, kidney, spleen, ovary, testis, thymus and the mammary gland of pregnant and lactating females (data not shown). Interestingly, neither the mouse nor the human gene was expressed in the mammary gland of virgin females. These RT-PCR results suggest that the tissue-specific regulation of the human gene under the control of its own promoter is similar to the endogenous mouse *Brca2* gene.

Expression was further examined in embryos, where expression of endogenous *Brca2* is first detected at E7.5 (Sharan et al., 1997). As development progresses, *Brca2* expression appears to be upregulated in cells that are rapidly dividing while reduced in cells undergoing differentiation. We examined the expression of the *BRCA2* transgene and compared it with the endogenous *Brca2* expression pattern in embryos at E9.5 by in situ hybridization. The human *BRCA2* gene was expressed in the developing embryo and the pattern of expression was identical to that of the endogenous *Brca2* gene (Fig. 2B-D). However, expression of the human *BRCA2* gene was reduced compared with the mouse gene. At E11.5 expression of both the human transgene and the mouse gene was found to be restricted to regions of rapid cell division (data not shown). From the expression pattern seen in the brain, both the mouse and the human genes were expressed in the neuroepithelium of the ventricular layer. Similar to E9.5 embryos, expression of the human *BRCA2* gene in E11.5 embryos was considerably lower than that of the endogenous gene. The qualitatively identical expression pattern of the mouse and human genes during embryogenesis provides insight into the viability of the *Brca2* homozygous mutant mice. Although the level of transcript expression is reduced, it must provide an amount of BRCA2 protein that is above the threshold level required for normal function during embryogenesis.

To assess further the expression of the human *BRCA2* transgene in testes and ovaries, we performed in situ hybridization with mouse *Brca2*- and human *BRCA2*-specific probes (Fig. 2). Although spermatocytes of 3-week old males showed high expression of the mouse gene (Fig. 2F), the human gene expression was barely above the background signal (Fig. 2G,H). In ovaries from a 3-week-old mouse, the endogenous *Brca2* gene was expressed in all the developing follicles as described previously (Fig. 2J), but there was lack of any specific signal of the transgene in these follicles (Blackshear et al., 1998). Similarly, in a 10-week-old ovary, expression of the endogenous mouse *Brca2* gene was detected in the oocyte and the surrounding granulosa cells but not in the corpora lutea, while the level of human *BRCA2* mRNA was not above background levels (Fig. 2N-P). The weak expression of the human *BRCA2* gene apparently did not lead to detectable protein expression, as we failed to observe the human BRCA2 protein in the ovaries and testes by immunohistochemistry (data not shown).

We conclude from these expression analyses that the infertility of the rescued animals is due to poor expression or function of the human BRCA2 protein in germ cells. Thus, the *Brca2 Ko/Ko; Tg* mice, in effect, are equivalent to a conditional knockout with respect to the gonads and can be used to study the function of BRCA2 in gametogenesis.

Male infertility phenotype

None of the four *Brca2 Ko/Ko; Tg/+* males produced any offspring after repeated mating for 2-6 months with either rescued or wild-type females, while their *Brca2 Ko/+; Tg/+* littermates sired multiple litters suggesting that the rescued males were infertile. To define further the infertility phenotype, the histology of the testes from males of different ages was examined. Testes of the rescued mutant males were small compared with controls. Histological examination of 3-week-old *Brca2 Ko/+; Tg/+* males revealed seminiferous tubules that were filled with spermatocytes (Fig. 3A). The rescued male testes also showed the presence of spermatocytes in seminiferous tubules but their number appeared reduced and some seminiferous tubules were completely devoid of germ cells (Fig. 3B). The seminiferous tubules of 2-month-old *Brca2 Ko/Ko; Tg/+* males appeared smaller compared with their normal littermate controls and showed interstitial cell hyperplasia (Fig. 3C,D). The Leydig cells appeared to be functionally normal as the weight of the seminal vesicles was unaffected in the mutant mice (data not shown). No germ cells beyond early meiotic prophase were present in the seminiferous tubules of the rescued males. Several tubules were completely devoid of germ cells and contained only Sertoli cells, suggesting that the germ cells were undergoing rapid degeneration. With germ cell deficiency, there was an increase in the relative number of Sertoli cells per seminiferous tubule in the mutants compared with the control tubules. The degeneration was more severe in 7-month-old rescued males, where very few seminiferous tubules had spermatocytes and majority of the tubules were filled with vacuolated Sertoli cells

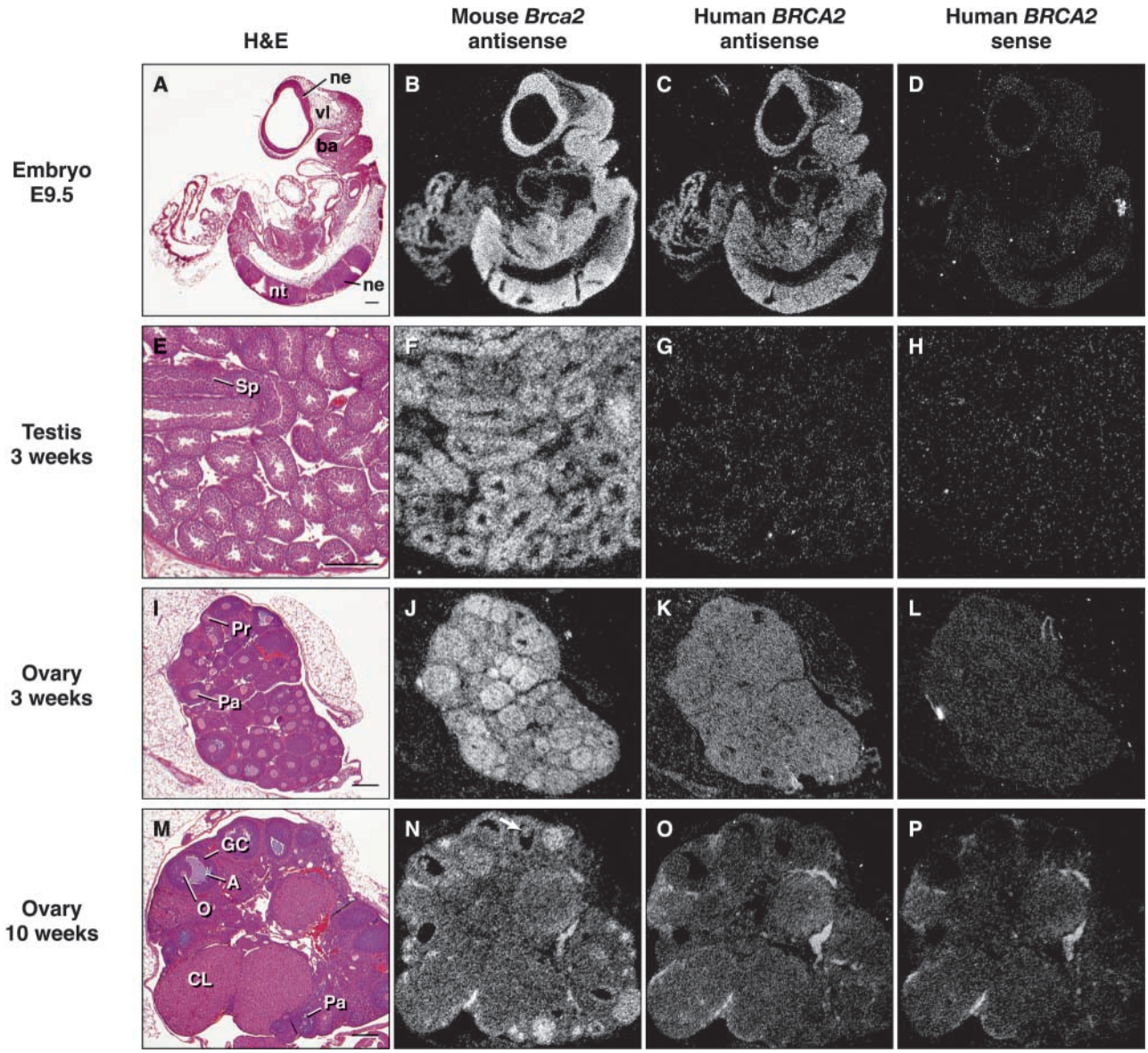

Fig. 2. In situ hybridization analyses comparing the expression of the human *BRCA2* transgene and endogenous mouse *Brca2*. (A-D) Sagittal sections of a E9.5 transgenic embryo. (E-H) Sections of the testis of a 3-week-old transgenic male. (I-L) Sections of the ovary of 3-week-old transgenic female. (M-P) Sections of the ovary of a 10-week-old transgenic female. (A,E,I M) Bright-field pictures of Hematoxylin and Eosin stained sections adjacent to those used in the in situ hybridization studies; (D,H,L,P) respective sections hybridized with human *BRCA2* sense probe as negative control. (B) Mouse *Brca2* expression is detected in the E9.5 embryo in the brain in the neuroepithelium of the ventricular region and the neural tube (first branchial arches). (C) The *BRCA2* transgene is expressed at reduced levels compared with the endogenous gene but the spatial expression pattern is identical to that of the endogenous gene. (F) *Brca2* expression is detected using antisense probe in the spermatocytes present in the seminiferous tubules. (G) The human *BRCA2* transgene expression is found at a level just above background. (J) In the ovary of a 3-week-old female, the mouse *Brca2* gene is found to be highly expressed in follicles at various stages of maturation. (K) No specific signal is observed in the follicles by human *BRCA2* antisense probe. (N) *Brca2* expression is detected in the follicles in granulosa cells and oocytes (arrow) of 10-week-old ovary. (O) Expression of the human transgene is not detected in the ovary. A, antral follicle; ba, branchial arch; CL, corpus lutea, GC, granulosa cells; ne, neuralepithelium; nt, neural tube; O, oocyte; Pa, preantral follicle; Pr, primary follicle; Sp, spermatocytes; vl, ventricular layer. Scale bars: 100 μm.

(Fig. 3E). The nuclei of these remaining spermatocytes appeared condensed and darkly stained.

To determine if the loss of germ cells from the seminiferous tubules was associated with cell death, the TdT-mediated fluorescein-dUTP nick-end-labeling (TUNEL) assay was used to detect the single and double strand DNA breaks that occur during apoptosis. Testes from 3-week-old rescued males were analyzed and compared with *Brca2 Ko/+; Tg* controls. Although very few TUNEL-positive spermatocytes were seen in the seminiferous tubules of control testis, the seminiferous tubules of the rescued animals had a large number of TUNEL-positive cells (Fig. 3F,G). This suggests that the BRCA2-

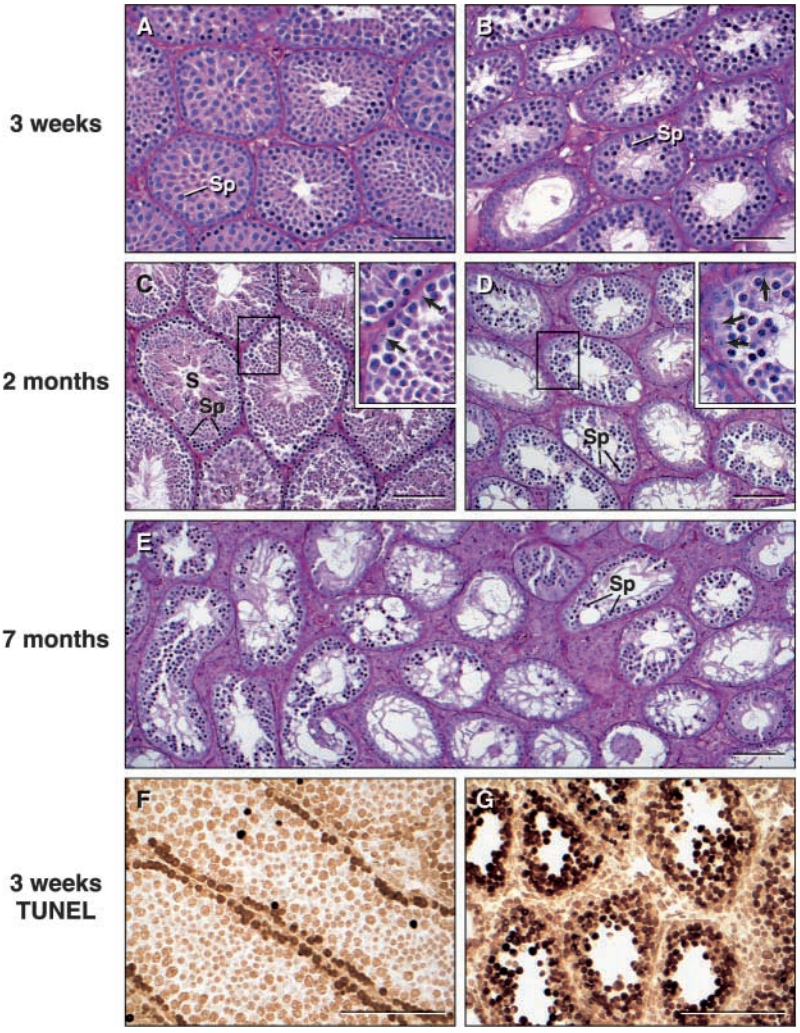

Fig. 3. Histology of testes at various ages. Testes from control (*Brca2 Ko/+; Tg/+*, A and C) and rescued males (*Brca2 Ko/Ko; Tg/+*, B,D,E) at 3 weeks (A,B), 2 months (C,D) and 7 months (E) of age were analyzed. (A,B) In young control males at 3 weeks of age, the seminiferous tubules are filled with spermatocytes. The rescued testes show presence of several seminiferous tubules with spermatocytes but there are few that have reduced number of spermatocytes. (C,D) At 2 months, adult male control testes contain spermatocytes at various stages of maturation as well as spermatozoa in the seminiferous tubules. In rescued males, the spermatocytes appear to be arrested in meiotic prophase I and no postmeiotic cells are visible. Several seminiferous tubules containing only Sertoli cells are observed. There appears to be a relative increase in the number of Sertoli cells per seminiferous tubule in the mutants (see insets, arrows indicate the Sertoli cells). (E) In rescued testes, by 7 months of age, most of the seminiferous tubules are completely devoid of germ cells and none contain normal looking spermatocytes, while control tubules exhibit normal spermatogenesis. (F,G) In rescued testes, there is an increase in apoptosis, as indicated by the TUNEL-positive staining cells (brown precipitate). Very few spermatocytes show brown staining in 3-week-old control males where as majority of the spermatocytes show positive staining in the rescued testes. In the control testis, some tubules show TUNEL-positive cells next to the basal lamina of the tubules, indicating that they are the spermatogonial cells. S, spermatozoa; Sp, spermatocytes. Scale bars: 50 μm.

deficient spermatocytes that are arrested in meiotic prophase undergo apoptosis, causing germ-cell depletion.

Analysis of meiotic progress in mutant males

As spermatocytes in testes of *Brca2 Ko/Ko; Tg/+* rescued animals appeared to be blocked during prophase I of meiosis, spermatocytes were examined by immunofluorescence with various antibodies to determine more precisely the timing of the block in prophase I. First, the localization of the endogenous mouse BRCA2 protein during normal meiosis was confirmed. As seen in Fig. 4A, signal for BRCA2 protein in zygotene spermatocytes is diffuse throughout the nucleus. As synapsis occurs in normal spermatocytes, BRCA2 staining begins to disappear and is no longer detected by the end of pachynema (data not shown) in accordance with previous findings (Chen et al., 1998). Mouse BRCA2 protein was not detected in *Brca2 Ko/Ko; Tg/+* spermatocytes (Fig. 4B). Similarly, no human BRCA2 protein was detected in either the heterozygous or homozygous mutant transgenic spermatocytes, confirming the negligible expression of the human protein in spermatocytes of transgenic mice (Fig. 4C,D).

The localization of synaptonemal complex protein SYCP3 (Dobson et al., 1994) in BRCA2-deficient spermatocytes revealed partial, but not complete synapsis of chromosomes, suggesting that the spermatocytes are blocked before or at the transition from zygonema to pachynema. To provide further evidence, we examined the expression of male germ-cell specific histone H1t protein, which appears during mid-pachynema (Cobb et al., 1999). Although the chromatin of control spermatocytes stains positively for histone H1t, the chromatin of spermatocytes in rescued mutants does not, suggesting arrest of both meiotic and spermatogenic developmental programs (Fig. 4E,F).

Events surrounding the initiation of meiotic recombination in the BRCA2-deficient spermatocytes were examined by determining the localization of two proteins known to be associated with the formation of recombination-related DNA double-strand breaks. First, we assessed the presence of SPO11, an evolutionarily conserved protein required for normal formation of meiosis-specific double strand breaks (Keeney et al., 1997). Positive staining for SPO11 protein was found in both *Brca2 Ko/Ko; Tg/+* and *Brca2 Ko/+; Tg/+* control spermatocytes (Fig. 4G,H). Second, we determined the presence of the phosphorylated form of histone H2AX (γ-H2AX), a marker for chromatin containing DNA double-strand breaks. *Brca2 Ko/Ko; Tg/+* spermatocytes show positive γ-H2AX staining, again suggesting that the chromatin in

BRCA2-deficient spermatocytes contains DNA with double-strand breaks. Normally, γ-H2AX staining disappears in pachynema, except for its localization with the sex chromosomes (Mahadevaiah et al., 2001). However, mutant spermatocytes do not exhibit either loss or re-localization of staining with anti-γ-H2AX, providing further evidence that they are blocked at a stage prior to pachynema.

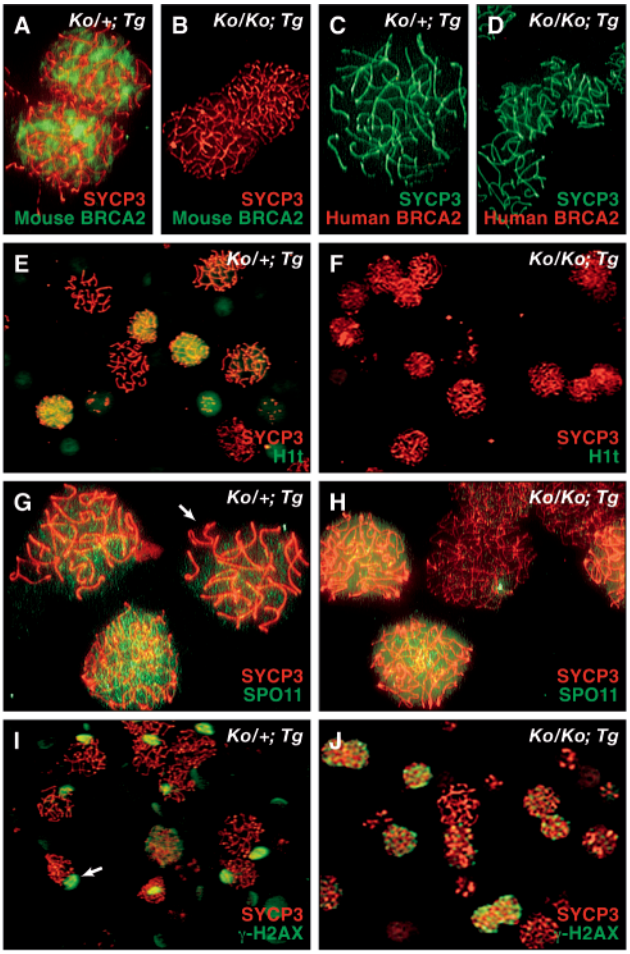

Fig. 4. Analysis by immunofluorescence of the localization of BRCA2, H1t, SPO11 and γ-H2AX proteins during male meiosis. Localization of these proteins was compared between control (*Brca2 Ko/+; Tg/+*, A,C,E,G,I) and rescued (*Brca2 Ko/Ko; Tg/+*, B,D,F,H,J) in preparations of surface-spread chromatin from spermatocytes. Nuclei were stained with antisera against SYCP3 (in red, except in C and D where SYCP3 is in green). (A) Mouse BRCA2 is present in the nuclei during zygonema, but (B) no signal is detected in the rescued spermatocytes as they lack a functional mouse *Brca2* gene. (C,D) The human protein is not detected in control or rescued spermatocytes. (E,F) Nuclei were examined for presence of male germ cell-specific, mid-pachytene marker, histone H1t. Control cells show positive staining but rescued cells lack the staining. (G,H) Both control and rescued spermatocytes exhibit expression of SPO11 protein during leptotene/zygotene stage, with diminished staining by pachynema in control spermatocytes (arrow). (I,J) Localization of phosphorylated histone H2AX (γ-H2AX), a marker for double-strand break formation, is seen in both genotypes. During pachytene stage, the staining of γ-H2AX disappears except in the sex chromosomes (arrow). Rescued spermatocytes do not show this typical pachytene staining pattern, further evidence that they do not reach this stage.

As BRCA2 interacts with RAD51 protein (Patel et al., 1998) and co-localizes with RAD51 in human spermatocytes (Chen et al., 1998), we examined localization of RAD51 protein and its meiosis-specific variant, DMC1, in BRCA2-deficient spermatocytes. Western blot analysis of the testes of *Brca2 Ko/Ko; Tg/+* mice showed presence of RAD51 and DMC1 proteins at levels similar to the control testes (data not shown). Interestingly, the number of RAD51 foci per nucleus was reduced in *Brca2 Ko/Ko; Tg/+* spermatocytes compared with heterozygous transgenic control spermatocytes (Fig. 5A-C). Analysis of RAD51 foci in mutant and control nuclei revealed that 98% of mutant spermatocytes in the leptotene and zygotene stages had reduced numbers of RAD51 foci (58% with no foci and majority of nuclei in 1-100 group had less than 10 foci and only a few had 20-30), while greater than 98% of control spermatocytes had 100-250 RAD51 foci per nuclei (Fig. 5C). Additionally, although many discrete DMC1 foci were visible over zygotene-stage spermatocytes in normal animals, few to no foci were detected in BRCA2-deficient spermatocytes, similar to the reduction seen in RAD51 foci (Fig. 5D,E). Finally, we examined the expression of replication protein A (RPA), a single-stranded DNA-binding protein involved in DNA replication and repair, which is associated with synapsed regions of the chromosomes during the zygotene and pachytene stages (Plug et al., 1997; Plug et al., 1998), and has been shown to interact with RAD51 (Golub, 1998). Surprisingly, despite reduced number of RAD51 foci and lack of extensive synapsis, we found abundant RPA foci present in mutant spermatocytes (Fig. 5F,G).

Female infertility phenotype and partial rescue by hormone treatment

To determine the phenotype of the BRCA2-deficient ovaries (obtained from the rescued females, *Brca2 Ko/Ko; Tg/+*), we examined their histology at various ages and compared them with the heterozygous transgenic ovaries (*Brca2 Ko/+; Tg/+*). Ovaries from postnatal day 2 (PND2) rescued females were morphologically similar to those from heterozygous transgenic females (Fig. 6A,B). Rescued female ovaries contained primordial and primary follicles and their number was similar to control ovaries. The ovaries of 3-week-old females also appeared indistinguishable from the littermate control ovaries (Fig. 6C,D). The rescued ovaries contained morphologically normal follicles in all stages of development. However, at this time point the number of primordial and primary follicles were eight- to tenfold reduced in the *Brca2 Ko/Ko; Tg/+* females (P=0.005 and 0.013, respectively, Fig. 6G). These data suggest massive loss in the oocyte pool between PND2 and 3 weeks. By contrast, there was no significant reduction in number of preantral follicles between the two genotypes (P=0.32). At 6 weeks of age, the rescued ovaries appeared smaller in size than heterozygous transgenic ovaries. The rescued ovaries contained follicles but their number was severely reduced (Fig. 6E,F). The follicles appeared degenerating and the surrounding layer of granulosa cells was poorly organized compared with follicles from ovaries of heterozygous transgenic littermates.

To determine if their infertility could be rescued by hormonal treatment, 6-week-old females were treated with pregnant mare serum gonadotropin (PMSG) to stimulate follicle maturation and with human chorionic gonadotropin (hCG) to initiate ovulation. The number of eggs was

significantly reduced in rescued females compared with controls (P=0.004). Although each heterozygous transgenic oviduct contained on an average 17.6±3.2 eggs (n=5), oviducts of rescued females contained 7.6±3.6 eggs (n=5). To determine the developmental potential of the oocytes, some of the superovulated females were mated with wild-type males following the hCG injection. The females were sacrificed after 12.5 days and the embryos were dissected from the uterine horns. Morphologically normal appearing embryos were harvested from some of the rescued females. However, the mean number of implanted embryos was 1.33±1.5 (n=3) compared with 14 (n=2) in control females. This suggested that the fertilization and/or developmental competence of the oocytes in the rescued mice were in some way compromised.

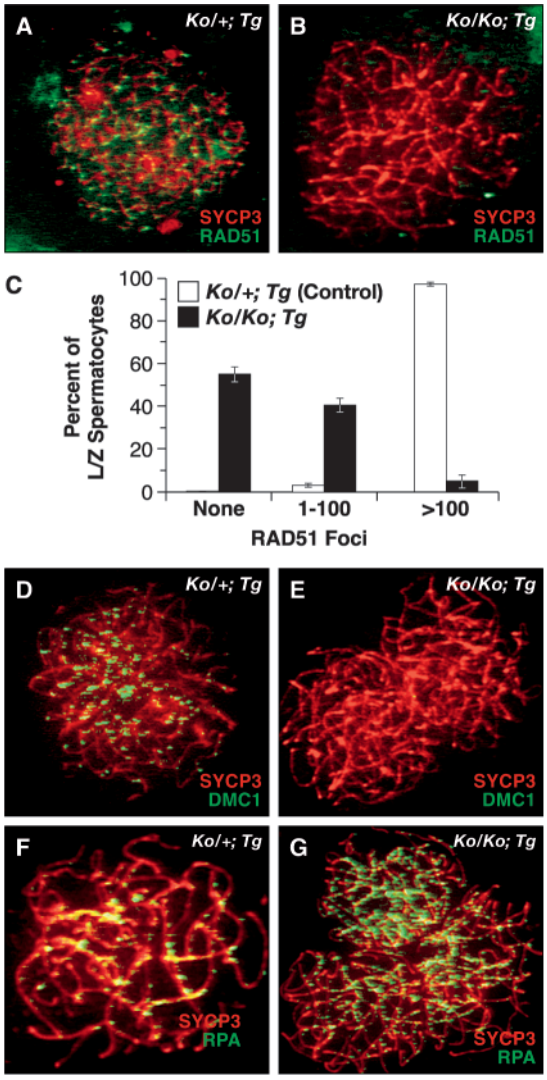

Fig. 5. Immunofluorescent analysis of localization of RAD51, DMC1 and RPA proteins (green) during male meiosis. Expression of these proteins was compared between control (*Brca2 Ko/+; Tg/+*, A,D, F) and rescued (*Brca2 Ko/Ko; Tg/+*, B,E,G) spermatocytes. Nuclei are also stained with SYCP3 antisera (in red). (A,B) RAD51 foci are visible on chromatin of control spermatocytes during the zygotene stage, but most of the rescued spermatocytes showed little or no RAD51 foci. (C) Semi-quantitative analysis of RAD51 foci per spermatocyte at the leptotene and zygotene stages reveals the reduction in number of foci in rescued spermatocytes. The majority of control spermatocytes had 100-250 foci per nuclei (>100 group). In the rescued spermatocytes, 58% had no foci while majority of nuclei in the 1-100 group had fewer than 10 foci, although a small number had 20-30 foci per nuclei. (D,E) Similar to RAD51, there is marked reduction in the number of DMC1 foci in rescued spermatocytes compared with control cells. (F,G) RPA protein is present in abundant foci in rescued spermatocytes compared with control spermatocytes.

Analysis of meiotic progress in mutant females

Because meiotic progress is arrested in mutant males, we hypothesized that there could be some abnormalities in meiosis in females as well. However, the presence of oocytes in young animals suggested that impairment to meiotic progress could be at a stage after the late prophase, or dictyate, arrest that normally occurs during female gametogenesis. Successful oocyte 'meiotic maturation' or progress through meiosis from prophase I to metaphase II is crucial for successful fertilization and embryo development.

To address our hypothesis, oocytes from control and rescued females were examined for their abilities to undergo meiotic maturation in vitro. Ninety GV-intact oocytes were collected from two control females (55 from a 9-week-old and 35 from a 7-week-old) and 31 oocytes were collected from two rescued females (21 from a 9-week-old and 10 from a 7-week-old), demonstrating that the rescued females had fewer germinal vesicle (GV)-intact oocytes than did the controls, as was anticipated from the ovarian histology. Additionally, the oocytes from rescued females showed a reduced ability to complete oocyte maturation successfully when compared with controls. GV-intact oocytes from control and rescued females were cultured for 16 hours in medium lacking dbcAMP to allow progression into meiosis from prophase I to metaphase II (Cho et al., 1974). Entry into meiosis is indicated by the breakdown of the nuclear envelope of the GV, known as GV breakdown (GVBD). Completion of the first stage of female meiosis (progression to metaphase II) is indicated by the emission of the first polar body (PB1), the product of asymmetric cytokinesis. As shown in Fig. 7, oocytes from the rescued females appeared capable of initiating meiotic maturation, as only 14% (4/29) remained arrested at GV stage after 16 hours of culture. However, abnormalities of meiotic maturation were observed; most notably, 21% (6/29) of the polar bodies appeared to be abnormally large, and a low number (9/29, 31%) had normal first polar bodies. It should be noted that the PB1 emission in the controls by 16 hours was relatively low (44%). Because oocytes of some strains of mice undergo meiotic maturation more slowly (Polanski, 1986), we cultured the oocytes that had begun maturation (59 controls, 25 rescued) for 3 additional hours, to 19 hours post-dbcAMP removal. In this time, ~50% of the GVBD oocytes in both the control and rescue groups progressed to emit the first polar body (Fig. 7B). To asses meiotic progress further, cells then were fixed and stained to label the F-actin and DNA (four out of the 59 control oocytes were lost in this process, and therefore data are reported for 55 oocytes.) Normal metaphase II-arrested eggs show first polar body (indicative of completion of meiosis I), chromatin arranged on the metaphase II plate and an actin-rich cap over the meiotic spindle (Fig. 8A). Although nearly 50% (12/25) of the rescued oocytes had this phenotype, abnormalities were observed in the others. The most common

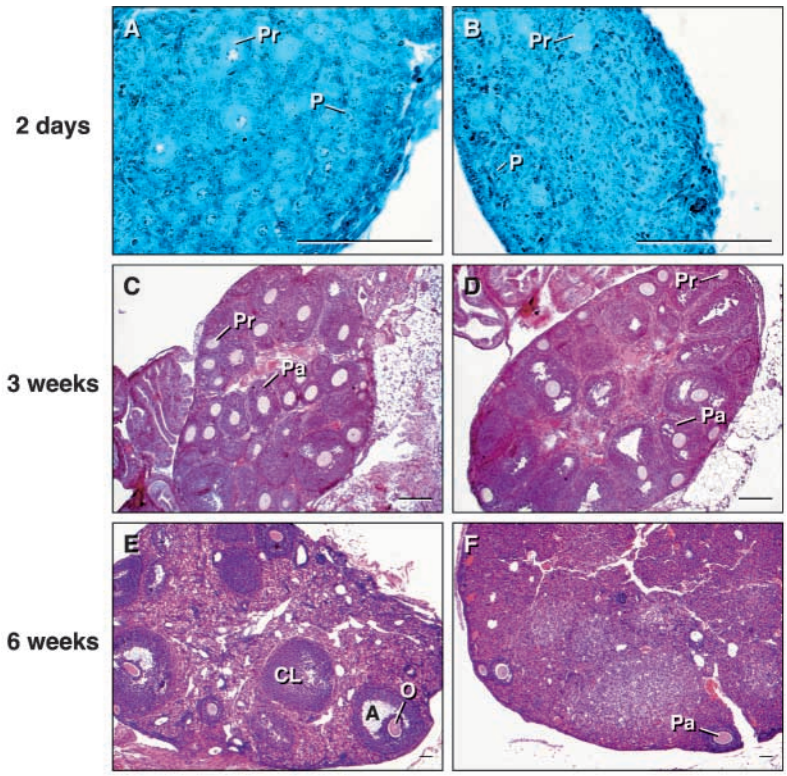

G

	Primordial	Primary	Preantral
Control Ovaries (n=4)	10,480 ± 2188	2,100 ± 442	6,200 ± 40
Rescued Ovaries (n=4)	1,220 ± 132	344 ± 234	4,556 ± 1,505

Fig. 6. Histology of ovaries obtained from control and rescued females at various ages. (A,C,E) Ovaries from control females (*Brca2 Ko/+; Tg/+*); (B,D,F) ovaries from rescued females (*Brca2 Ko/Ko; Tg/+*). (A,B) Ovaries from postnatal day 2 females stained with Weigert's Hematoxylin-picric acid Methyl Blue; (C,D) Three-week-old females; (E,F) Six-week-old females. The 3- and 6-week-old ovary sections are stained with Hematoxylin and Eosin. A marked reduction in the follicles was seen in the 6-week-old rescued ovaries. CL, corpus lutea; P, primordial follicles; Pr, primary follicles; Pa, preantral follicles; A, antral follicles; O, oocyte. Scale bars: 50 μm. (G) Table shows the number of follicles found in 3-week-old control and rescued female ovaries. The number of primordial and primary follicles were significantly reduced in rescued females.

anomaly was an oversized polar body-like structure (7/25, 28%; Fig. 8B,C). While eggs with large polar bodies have been observed in some instances of female meiosis abnormalities (e.g. the Mos-deficient and endothelial nitric oxide synthase-deficient mice (Choi et al., 1996; Jablonka-Shariff and Olson, 1998), the eggs with oversized polar body-like structures observed here were different. In the majority of these eggs (6/7), all of the DNA was in the PB-like structures and no DNA present in the oocyte (Fig. 8B,C). Other abnormalities in the oocytes from rescued females included apparent impairment of the first meiotic division, including abnormal chromatin condensation (Fig. 8D), chromatin condensation but little organization of the metaphase I spindle (Fig. 8E), formation of a metaphase I spindle but failure to emit PB1 (Fig. 8F), or failure to progress to metaphase II and instead of having an abnormal, tightly condensed chromatin 'wad' in an egg that had emitted PB1 (Fig. 8G). By contrast, 85% (47/55) of the control oocytes emitted the first polar body and 71% (39/55) showed proper metaphase II arrest. The other eight control cells with PB1s had slight metaphase II abnormalities, namely incomplete chromosome congression to the metaphase II spindle (Fig. 8H). Of the eight control oocytes that had undergone GVBD but not emitted PB1, seven of these appeared to be normal metaphase I cells, with the meiotic spindle positioned at the periphery of the cell.

Discussion

A unique mouse model, deficient for endogenous BRCA2 protein, but carrying a BAC containing the human *BRCA2* gene, rescues the embryonic lethality of *Brca2*-null mice. In spite of poor sequence identity, the genetic complementation of a mutation in the mouse *Brca2* gene by the human *BRCA2* transgene sheds light on conservation of function of the mouse and human proteins (Sharan and Bradley, 1997). Similar functional conservation was described for the human *BRCA1* gene, which can fully complement the *Brca1* mutant phenotype (Lane et al., 2000; Chandler et al., 2001). For reasons not known, the human *BRCA2* transgene is poorly expressed in gonads with ensuing infertility. The infertility of the rescued mice is due to loss of endogenous BRCA2 protein function and not to any detrimental effect of the BAC, as the *Brca2 Ko/+; Tg/+* mice are fertile even though they have the same copy number of the BAC transgene as the *Brca2 Ko/Ko; Tg/+* mice. This model provides evidence for key roles of BRCA2 protein in both male and female gametogenesis, particularly in the meiotic stages. Interestingly, the meiotic phenotype of BRCA2 protein deficiency is variable: in males there is arrest of meiosis in early prophase, while in females some oocytes are capable of progressing through the meiotic division phase and giving rise to embryos, although with a high frequency of abnormalities.

Previously, the expression of BRCA2 protein in adult testes and ovaries and its colocalization with RAD51 on synapsed chromosomes in spermatocytes had suggested a role for this protein in meiosis (Chen et al., 1998), but this was difficult to test experimentally because of the lethality of *Brca2*-null embryos and the early germ-cell loss in mice homozygous for either of the two hypomorphic alleles of *Brca2* (Connor et al., 1998; Friedman et al., 1998). Here, we have circumvented these problems by showing that *Brca2*-null mice rescued by a human *BRCA2* transgene survive to adulthood, but with impaired germ-cell development. As the human *BRCA2* transgene is poorly expressed in the gonads and human protein could not be detected in ovaries or testes, we presume that infertility results from BRCA2 deficiency in the gonads, especially in the germ cells.

The phenotype of spermatocytes in *Brca2 Ko*/*Ko*; *Tg*/+ males reveals a requirement for adequate levels of BRCA2 protein for normal meiotic prophase progression, including

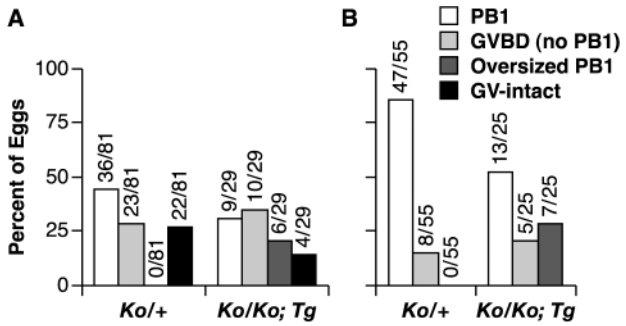

Fig. 7. Results of in vitro maturation of oocytes. GV-intact oocytes were collected from control and rescued female mice and allowed to undergo meiotic maturation in vitro. (A,B) The percentages of oocytes that had emitted the first polar body (PB1), undergone germinal vesicle breakdown (GVBD) but not emitted the first polar body, emitted an oversized polar body (oversized PB1), or remained GV-intact after 16 hours (A) or 19 hours (B). Values above the bars show the actual numbers of oocytes with the given appearance per total number of oocytes in a group.

assembly of protein complexes onto chromosomal axes. Although synapsis is initiated in BRCA2-deficient spermatocytes, it is never completed and mutant spermatocytes do not reach the pachytene stage of meiotic prophase. The presence of both of SPO11 and γ-H2AX proteins on chromatin of mutant spermatocytes suggests that early recombination-related DNA double-strand break formation probably occurs in BRCA2-deficient spermatocytes. However, recombination complexes of RAD51 and DMC1 are not appropriately assembled onto meiotic chromosomal axes in the absence of BRCA2 protein. Thus, the role of BRCA2 in meiotic recombination could be similar to that hypothesized for double-strand break repair in mitotic cells, where it is thought that BRCA2 recruits RAD51 to sites of DNA damage, thus initiating repair (Davies et al., 2001). The BRCA2 protein may also be directly or indirectly responsible for recruiting DMC1 protein to meiotic chromosomal axes at the site of RAD51 foci, as DMC1 localization was dramatically diminished in mutant spermatocytes. In normal spermatocytes, RAD51 and DMC1 colocalize and interact with SYCP3 (Tarsounas et al., 1999),

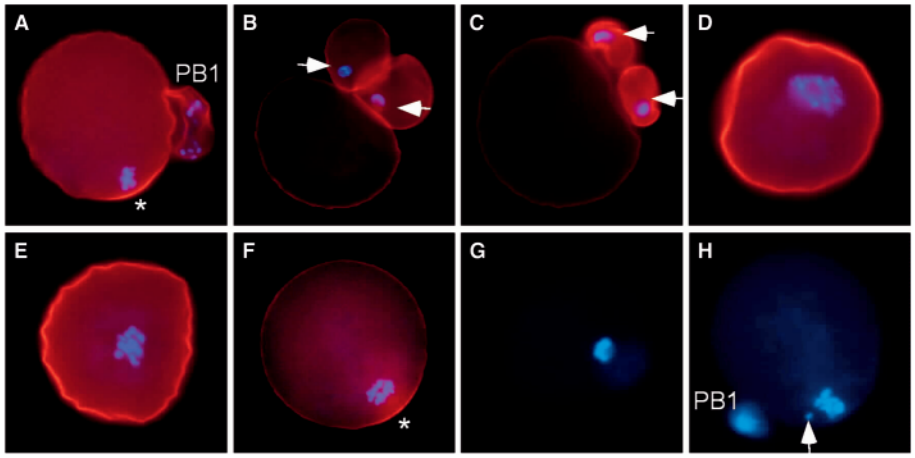

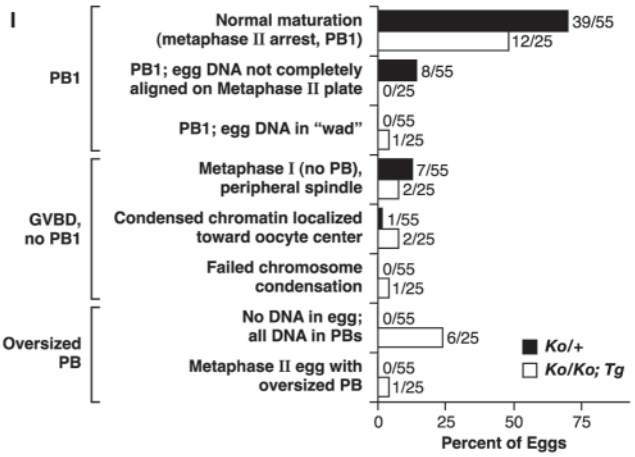

Fig. 8. Phenotypes of oocytes after in vitro maturation. Examples of the various phenotypes observed in matured control and rescued oocytes (red labeling indicates F-actin detected by phalloidin, and blue labeling indicates DNA detected by DAPI). (A) Normal mature 'PB1' egg, with the first polar body emitted (indicated by PB1) and the egg chromosomes organized on the metaphase II spindle. An actin-rich cap overlies the meiotic spindle (asterisk). (B,C) Two examples of 'oversized polar body' phenotype. Twenty-eight percent (7/25) of the rescued eggs had this phenotype, and in six of these seven, all of the DNA was present in the polar body-like structures (arrows), with no DNA present in the egg. These polar body-like structures ranged in size from very large, containing approximately one-third of the oocyte cytoplasm (B) to somewhat more normal in size (C; compare with A). (D) An oocyte that has undergone GVBD but not emitted PB1, with chromatin near the center of the egg that appears to have failed to condense properly. In this cell, there is no actin-rich cap and instead the actin is symmetrically localized around the cell cortex, as it is in a GV-intact oocyte. (E) An oocyte that has undergone GVBD but not emitted PB1, with condensed chromatin that remains near the center of the egg (rather than having migrated to the cell periphery). This DNA appears to be poorly organized, not organized on a metaphase I spindle. As in the cell in D, the actin in this cell is symmetrically localized. (F) An oocyte that has undergone GVBD but not emitted PB1, with the metaphase I spindle having migrated to the cell periphery. The asterisk indicates the actin-rich cap over the metaphase I spindle. This oocyte appears poised to undergo PB1 emission; it is not clear if it was arrested at this stage or was simply slower than the rest of its cohort. (G) An egg that has emitted PB1 (out of the plane of focus of this image), but the egg DNA looks abnormal, as a tightly condensed wad of DNA rather than chromosomes organized on the metaphase II spindle. (Only the DAPI staining in shown in this image to show the DNA wad more clearly.) (H) A nearly normal metaphase II egg, except the chromosomes are not completely aligned on the metaphase II plate; the arrowhead indicates chromatin cluster that is not aligned. (Only the DAPI staining in shown in this image, in order to show the straggler chromosome more clearly.) (I) Percentages of the control and rescued oocytes that displayed each of the eight observed phenotypes after 19 hours in culture medium lacking dbcAMP. Values over the bars indicate the actual numbers of oocytes per total control or rescued oocytes that displayed that phenotype.

suggesting functional interaction of these proteins in recombination events. The presence of RAD51 foci in DMC1-deficient spermatocytes (Pittman et al., 1998; Yoshida et al., 1998) implies that DMC1 is not required for localization of RAD51 onto chromosomal axes. However, the role of RAD51 in DMC1 recruitment to chromatin is not known, as there is early embryonic lethality of *Rad51*-null mice (Lim and Hasty, 1996; Tsuzuki et al., 1996). Hence, the reduced number of DMC1 foci in BRCA2-deficient spermatocytes could be because of lack of BRCA2 or because of failure of RAD51 to load onto chromatin. In spite of greatly diminished RAD51 and DMC1 localization in BRCA2-deficient spermatocytes, numerous foci of RPA are found on chromosomal axes. RPA and RAD51 do not always colocalize in spermatocytes (Tarsounas and Moens, 2001) and the pattern of RPA localization in BRCA2-deficient spermatocytes suggests that neither BRCA2 nor RAD51 may be required for RPA localization on chromosomal axes, but that BRCA2- or RAD51-mediated processes could be required for removal of RPA from chromosomal axes. Taken together, these observations of BRCA2-deficient spermatocytes suggest a pivotal role for BRCA2 protein in organizing the complex of proteins that assemble onto chromosomal axes during early meiotic prophase. Additionally, the failure of spermatocytes to progress in their developmental program suggests a strong dependency upon completion of early events of recombination.

Although it is not known if absence of BRCA2 protein can cause some prophase arrest of oocytes, it is clear that some oocytes survive and progress to the end of meiotic prophase, where they become normally arrested. Thus, there is sexual dimorphism between spermatocytes and oocytes in their dependency on BRCA2-mediated meiotic events. However, the fact that we do detect the human *BRCA2* transcript by RT-PCR in the gonads, the possibility that some human protein may be present cannot be ruled out. This level may be beyond the level of detection by immunohistochemistry but may be sufficient to partially rescue the phenotype. Therefore, the possibility that a low level of BRCA2 protein in the ovary might be sufficient for meiotic maturation in females but not in males cannot be ruled out. Nonetheless, oocyte survival, the progress of oogenesis and acquisition of meiotic competence is indeed compromised by the absence of BRCA2; there is a marked reduction in the number of oocytes in the rescued females. Even though the rescued females appear to make some normal GV-intact, diplotene oocytes, multiple abnormalities are seen in oocytes undergoing maturation in vitro. Additionally, after gonadotropin treatment, there were 2.5-fold fewer metaphase II eggs from the BRCA2-deficient females compared with the controls, and 10-fold fewer E12.5 embryos in rescued females compared with the controls. These analyses of both in vitro and in vivo maturation, fertilization and embryogenesis suggest that the oocytes from rescued BRCA2-deficient females have reduced competence to undergo maturation and fertilization and to support embryonic development. Taken together, these abnormalities reveal a complex role for BRCA2 in oogenesis, and raise the possibility that all oocytes might be abnormal, but some escape arrest of development.

Thus, aspects of the meiotic phenotype of BRCA2 deficiency appear sexually dimorphic: spermatocytes arrest in early meiotic prophase, while at least some oocytes survive to the end of meiotic prophase, but many exhibit abnormalities of subsequent maturation and developmental competence. Similar sexually dimorphic phenotypes have been observed for many meiotic mutations (Hunt and Hassold, 2002). Interestingly, these include many of those mutations where the male phenotype is meiotic arrest at or around the transition from zygonema to pachynema: *Brca2* (this report), *Msh4* (Kneitz et al., 2000), *Scp3* (Yuan et al., 2000; Yuan et al., 2002) and *Mei1* (Libby et al., 2002); in these mutant female mice, oocytes can progress through meiotic prophase. Taken together, these phenotypes reveal profound differences between male and female meiosis in mice. At the moment, it is not possible to discriminate between two alternative explanations: either the mechanics of meiosis differ between sexes in such a way that the relevant proteins are not required for recombination and meiotic progress in oocytes or meiotic checkpoints present in spermatocytes are lacking or inefficient in oocytes.

The phenotype of the rescued *Brca2* mutant mice suggests that human *BRCA2*-mutation carriers could also be predisposed to fertility problems. In one recent study (Vachon et al., 2002), individuals with a family history of breast and ovarian cancer were found to be at risk for nulliparity. Thus, given the proposed role of BRCA2 in DNA repair in somatic as well as germ cells, cancer predisposition and infertility may represent two different tissue-specific phenotypes of mutation in a single gene, more fully revealing its function.

We thank Drs Allan Bradley, Neal Copeland, John Eppig, Amy Inselman, Bruce McKee and Sundar Venkatachalam for helpful discussions and critical review of the manuscript; Madalena Tarsounas and Stephen West for DMC1 antibody; Jairaj Acharya for help with the TUNEL assay; Keith Rogers and his group in the Histotechnology Laboratory for excellent technical assistance; Dr Dahlem Smith for help with histopathological analysis; and Richard Frederickson of the Publication Department for the illustrations. This research was supported by the National Cancer Institute, the Department of Health and Human Services (S.K.S. and L.T.), National Institutes of Health grants HD 37696 (J.P.E.), HD 38955 (J.A.F.) and HD 33816 (M.A.H.).

References

Blackshear, P. E., Goldsworthy, S. M., Foley, J. F., McAllister, K. A., Bennett, L. M., Collins, N. K., Bunch, D. O., Brown, P., Wiseman, R. W. and Davis, B. J. (1998). Brca1 and Brca2 expression patterns in mitotic and meiotic cells of mice. *Oncogene* **16**, 61-68.

Bork, P., Blomberg, N. and Nilges, M. (1996) Internal repeats in the brca2 protein sequence. *Nat. Genet.* **13**, 22-23.

Chandler, J., Hohenstein, P., Swing, D. A., Tessarollo, L. and Sharan, S. K. (2001). Human BRCA1 gene rescues the embryonic lethality of Brca1 mutant mice. *Genesis* **29**, 72-77.

Chen, J., Silver, D. P., Walpita, D., Cantor, S. B., Gazdar, A. F., Tomlinson, G., Couch, F. J., Weber, B. L., Ashley, T., Livingston, D. M. and Scully, R. (1998). Stable interaction between the products of the BRCA1 and BRCA2 tumor suppressor genes in mitotic and meiotic cells. *Mol. Cell* **2**, 317-328.

Cho, W. K., Stern, S. and Biggers, J. D. (1974). Inhibitory effect of dibutyryl cAMP on mouse oocyte maturation in vitro. *J. Exp. Zool.* **187**, 383-386.

Choi, T. S., Fukasawa, K., Zhou, R. P., Tessarollo, L., Borror, K., Resau, J. and Vande Woude, G. F. (1996). The Mos/mitogen-activated protein kinase (MAPK) pathway regulates the size and degradation of the first polar body in maturing mouse oocytes. *Proc. Natl. Acad. Sci. USA* **93**, 7032-7035.

Cobb, J., Reddy, R. K., Park, C. and Handel, M. A. (1997). Analysis of expression and function of topoisomerase I and II during meiosis in male mice. *Mol Reprod. Dev.* **46**, 489-498.

Cobb, J., Cargile, B. and Handel, M. A. (1999). Acquisition of competence to condense metaphase I chromosomes during spermatogenesis. *Dev. Biol.* **205**, 49-64.

Connor, F., Bertwistle, D., Mee, P. J., Ross, G. M., Swift, S., Grigorieva,

E., Tybulewicz, V. L. and Ashworth, A. (1998). Tumorigenesis and a DNA repair defect in mice with a truncating *Brca2* mutation. *Nat. Genet.* **17**, 423-430.

Davies, A. A., Masson, J. Y., McIlwraith, M. J., Stasiak, A. Z., Stasiak, A., Venkitaraman, A. R. and West, S. C. (2001). Role of BRCA2 in control of the RAD51 recombination and DNA repair protein. *Mol. Cell* **7**, 273-282.

Dobson, M. J., Pearlman, R. E., Karaiskakis, A., Spyropoulos, B. and Moens, P. B. (1994). Synaptonemal complex proteins: occurrence, epitope mapping and chromosome disjunction. *J. Cell Sci.* **107**, 2749-2760.

Eaker, S., Pyle, A., Cobb, J. and Handel, M. A. (2001). Evidence for meiotic spindle checkpoint from analysis of spermatocytes from Robertsonian-chromosome heterozygous mice. *J. Cell Sci.* **114**, 2953-2965.

Evans, J. P., Foster, J. A., McAvey, B. A., Gerton, G. L., Kopf, G. S. and Schultz, R. M. (2000). The effects of perturbation of cell polarity on molecular markers of sperm-egg binding sites on mouse eggs. *Biol. Reprod.* **62**, 76-84.

Friedman, L. S., Thistlethwaite, F. C., Patel, K. J., Yu, V. P., Lee, H., Venkitaraman, A. R., Abel, K., Carlton, M. B., Hunter, S. M., Colledge, W. H. et al. (1998). Thymic lymphomas in mice with a truncating mutation in Brca2. *Cancer Res.* **58**, 1338-1343.

Golub, E. I., Gupta, R. C., Haaf, T., Wold, M. S. and Radding, C. M. (1998). Interaction of human rad51 recombination protein with single-stranded DNA binding protein, RPA. *Nucleic Acids Res.* **26**, 5388-5393.

Hakem, R., de la Pompa, J. L. and Mak, T. W. (1998). Developmental studies of Brca1 and Brca2 knock-out mice. *J. Mamm. Gland Biol. Neoplasia* **3**, 431-445.

Hogan, B., Beddington, R., Constantini, F. and Lacy, E. (1994). *Manipulating the Mouse Embryo A Laboratory Manual*, 2nd edn. Cold Spring Harbor, NY: Cold Spring Harbor Laboratory Press.

Hunt, P. A. and Hassold, T. J. (2002). Sex matters in meiosis. *Science* **296**, 2181-2183.

Jablonka-Shariff, A. and Olson, L. M. (1998). The role of nitric oxide in oocyte meiotic maturation and ovulation: meiotic abnormalities of endothelial nitric oxide synthase knock-out mouse oocytes. *Endocrinology* **139**, 2944-2954

Keeney, S., Giroux, C. N. and Kleckner, N. (1997). Meiosis-specific DNA double-strand breaks are catalyzed by Spo11, a member of a widely conserved protein family. *Cell* **88**, 375-384.

Kneitz, B., Cohen, P. E., Avdievich, E., Zhu, L., Kane, M. F., Hou, H. Jr, Kolodner, R. D., Kucherlapati, R., Pollard, J. W. and Edelmann, W. (2000). MutS homolog 4 localization to meiotic chromosomes is required for chromosome pairing during meiosis in male and female mice. *Genes Dev.* **14**, 1085-1097.

Lane, T. F., Lin, C., Brown, M. A., Solomon, E. and Leder, P. (2000). Gene replacement with the human BRCA1 locus: tissue specific expression and rescue of embryonic lethality in mice. *Oncogene* **19**, 4085-4090.

Libby, B. J., de la Fuente, R., O'Brien, M. J., Wigglesworth, K., Cobb, J., Inselman, A., Eaker, S., Handel, M. A., Eppig, J. J. and Schimenti, J. C. (2002). The mouse meiotic mutation mei1 disrupts chromosome synapsis with sexually dimorphic consequences for meiotic progression. *Dev. Biol.* **242**, 174-187.

Lim, D. S. and Hasty, P. (1996). A mutation in mouse rad51 results in an early embryonic lethal that is suppressed by a mutation in p53. *Mol. Cell Biol.* **16**, 7133-7143.

Mahadevaiah, S. K., Turner, J. M., Baudat, F., Rogakou, E. P., de Boer, P., Blanco-Rodriguez, J., Jasin, M., Keeney, S., Bonner, W. M. and Burgoyne, P. S. (2001). Recombinational DNA double-strand breaks in mice precede synapsis. *Nat. Genet.* **27**, 271-276.

Masson, J. Y., Davies, A. A., Hajibagheri, N., van Dyck, E., Benson, F. E., Stasiak, A. Z., Stasiak, A. and West, S. C. (1999). The meiosis-specific recombinase hDmc1 forms ring structures and interacts with hRad51. *EMBO J.* **18**, 6552-6560.

Patel, K. J., Yu, V. P., Lee, H., Corcoran, A., Thistlethwaite, F. C., Evans, M. J., Colledge, W. H., Friedman, L. S., Ponder, B. A. and Venkitaraman, A. R. (1998). Involvement of Brca2 in DNA repair. *Mol. Cell* **1**, 347-357.

Pittman, D. L., Cobb, J., Schimenti, K. J., Wilson, L. A., Cooper, D. M., Brignull, E., Handel, M. A. and Schimenti, J. C. (1998). Meiotic prophase arrest with failure of chromosome synapsis in mice deficient for *Dmc1*, a germline-specific RecA homolog. *Mol. Cell* **1**, 697-705.

Plug, A. W., Peters, A. H., Xu, Y., Keegan, K. S., Hoekstra, M. F., Baltimore, D., de Boer, P. and Ashley, T. (1997). ATM and RPA in meiotic chromosome synapsis and recombination. *Nat. Genet.* **17**, 457-461.

Plug, A. W., Peters, A. H., Keegan, K. S., Hoekstra, M. F., de Boer, P. and Ashley, T. (1998). Changes in protein composition of meiotic nodules during mammalian meiosis. *J. Cell Sci.* **111**, 413-423.

Polanski, Z. (1986). In-vivo and in-vitro maturation rate of oocytes from two strains of mice. *J. Reprod. Fertil.* **78**, 103-109.

Polanski, Z., Ledan, E., Brunet, S., Louvet, S., Verlhac, M. H., Kubiak, J. Z. and Maro, B. (1998). Cyclin synthesis controls the progression of meiotic maturation in mouse oocytes. *Development* **125**, 4989-4997.

Rahman, N. and Stratton, M. R. (1998). The genetics of breast cancer susceptibility. *Annu. Rev. Genet.* **32**, 95-121.

Rajan, J. V., Wang, M., Marquis, S. T. and Chodosh, L. A. (1996). Brca2 is coordinately regulated with Brca1 during proliferation and differentiation in mammary epithelial cells. *Proc. Natl. Acad. Sci. USA* **93**, 13078-13083.

Sharan, S. K. and Bradley, A. (1997). Murine *Brca2*: sequence, map position and expression pattern. *Genomics* **40**, 234-241.

Sharan, S. K., Morimatsu, M., Albrecht, U., Lim, D. S., Regel, E., Dinh, C., Sands, A., Eichele, G., Hasty, P. and Bradley, A. (1997). *Brca2* deficiency in mice results in embryonic lethality and rad51-mediated radiation hypersensitivity. *Nature* **386**, 804-810.

Smith, B. J., Plowchalk, D. R., Sipes, I. G. and Mattison, D. R. (1991). Comparison of random and serial sections in assessment of ovarian toxicity. *Reprod. Toxicol.* **5**, 379-383.

Tarsounas, M., Morita, T., Pearlman, R. E. and Moens, P. B. (1999). RAD51 and DMC1 form mixed complexes associated with mouse meiotic chromosome cores and synaptonemal complexes. *J. Cell Biol.* **147**, 207-220.

Tarsounas, M. and Moens, P. B. (2001). Checkpoint and DNA-repair proteins are associated with the cores of mammalian meiotic chromosomes. *Curr. Top. Dev. Biol.* **51**, 109-134.

Tavtigian, S. V., Simard, J., Rommens, J., Couch, F., Shattuck-Eidens, D., Neuhausen, S., Merajver, S., Thorlacius, S., Offit, K., Stoppa-Lyonnet, D. et al. (1996). The complete *BRCA2* gene and mutations in chromosome. *Nat. Genet.* **12**, 333-337.

Tessarollo, L. and Parada, L. F. (1995). In situ hybridization. In *Oncogene Techniques* (ed. P. K. Vogt and I. M. Verma) *Methods in Enzymology*, Vol. 254, pp. 419-430. San Diego, CA: Academic Press.

Tsuzuki, T., Fujii, Y., Sakumi, K., Tominaga, Y., Nakao, K., Sekiguchi, M., Matsushiro, A., Yoshimura, Y. and Morita, T. (1996). Targeted disruption of the Rad51 gene leads to lethality in embryonic mice. *Proc. Natl. Acad. Sci. USA* **93**, 6236-6240.

Vachon, C. M., Mink, P. J., Janney, C. A., Sellers, T. A., Cerhan, J. R., Hartmann, L. and Folsom, A. R. (2002). Association of parity and ovarian cancer risk by family history of breast or ovarian cancer in a population-based study of postmenopausal women. *Epidemiology.* **13**, 66-71.

Vaughn, J. P., Cirisano, F. D., Huper, G., Berchuck, A., Futreal, P. A., Marks, J. R. and Iglehart, J. D. (1996). Cell cycle control of BRCA2. *Cancer Res.* **56**, 4590-4594.

Venkitaraman, A. R. (2002). Cancer susceptibility and the functions of BRCA1 and BRCA2. *Cell* **108**, 171-182.

Wong, A. K. C., Pero, R., Ormonde, P. A., Tavtigian, S. V. and Bartel, P. L. (1997). RAD51 interacts with the evolutionarily conserved BRC motifs in the human breast cancer susceptibility gene *BRCA2*. *J. Biol. Chem.* **272**, 31941-31944.

Wooster, R., Bignell, G., Lancaster, J., Swift, S., Seal, S., Mangion, J., Collins, N., Gregory, S., Gumbs, C. and Micklem, G. (1995). Identification of the breast cancer susceptibility gene *BRCA2*. *Nature* **378**, 789-792.

Yang, H., Jeffrey, P. D., Miller, J., Kinnucan, E., Sun, Y., Thoma, N. H., Zheng, N., Chen, P. L., Lee, W. H. and Pavletich, N. P. (2002). BRCA2 Function in DNA binding and recombination from a BRCA2-DSS1-ssDNA structure. *Science* **297**, 1837-1848.

Yoshida, K., Kondoh, G., Matsuda, Y., Habu, T., Nishimune, Y. and Morita, T. (1998). The mouse RecA-like gene *Dmc1* is required for homologous chromosome synapsis during meiosis. *Mol. Cell* **1**, 707-718.

Yuan, L., Liu, J. G., Zhao, J., Brundell, E., Daneholt, B. and Hoog, C. (2000). The murine SCP3 gene is required for synaptonemal complex assembly, chromosome synapsis, and male fertility. *Mol. Cell.* **5**, 73-83.

Yuan, L., Liu, J. G., Hoja, M. R., Wilbertz, J., Nordqvist, K. and Hoog, C. (2002). Female germ cell aneuploidy and embryo death in mice lacking the meiosis-specific protein SCP3. *Science* **296**, 1115-1118.

Zabludoff, S. D., Wright, W. W., Harshman, K. and Wold, B. J. (1996). BRCA1 mRNA is expressed highly during meiosis and spermiogenesis but not during mitosis of male germ cells. *Oncogene* **13**, 649-653.